

PHOTOCHEMISTRY
AND MAGNETOCHEMISTRY

Preparation and Photophysical Properties of Thin Films of Coumarin Dyes

N. Kh. Ibrayev^a, E. V. Seliverstova^a, V. I. Alekseeva^b, L. E. Marinina^b, and L. P. Savvina^b

^aInstitute of Molecular Photonics, Buketov Karaganda State University, Karaganda, 100028 Kazakhstan

^bState Scientific Center of the Russian Federation (NIOPiK), Moscow, 103787 Russia

e-mail: niazibaev@mail.ru

Received June 14, 2012

Abstract—The results from investigating the photophysical properties of new coumarin dyes synthesized and incorporated into Langmuir–Blodgett films are presented. A method for forming monolayers on the surface of a water/air interface is proposed. The phase states of mixed monolayers on a water surface are studied. It is found that mixed monolayers of amphiphilic polyampholyte and dye allow us to obtain more stable and condensed films, relative to films of single components. The spectral and luminescent properties of synthesized dyes in solution and in Langmuir–Blodgett films are studied.

Keywords: coumarin dyes, properties, Langmuir–Blodgett films.

DOI: 10.1134/S0036024413070133

INTRODUCTION

Langmuir–Blodgett (LB) technology finds wide application in preparing mono- and polylayers of organic molecules, molecular complexes, metal nanostructures, and photonic crystals [1]. Of fundamental importance to LB technology is the possibility of controlling structure at the molecular level. Classical LB technology employs amphiphilic molecules that allow us to form monolayers with regular arrangements of particles on a water/air interface. A monolayer can be repeatedly transferred onto the surface of a solid support, thereby obtaining multilayered films. Thin solid films with mixed monolayers of aliphatic acids and nonamphiphilic organic molecules can be prepared by using the LB technique [2–5]. There are many examples of preparing LB films around surface active polymeric materials, which have better parameters of thermal and mechanical strength than films based on aliphatic acids [6–8].

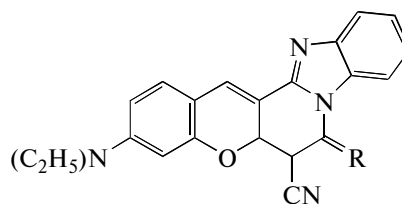
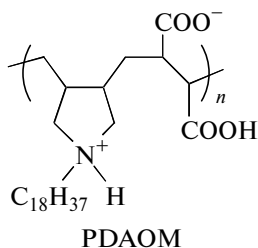
Coumarin derivatives exhibit intense fluorescence in the blue–green area of the spectrum and thus find use in tunable lasers, in dyes [9], in nonlinear optics [10, 11], and as luminescent probes [12]. Coumarins of flexible structure are sensitive to medium polarity, owing to intramolecular charge transfer [13].

This work presents our results from investigating the photophysical properties of new coumarin synthesized dyes (chromens **I** and **II**) incorporated into LB layers of the amphiphilic polyampholyte polymer poly(*N,N*-diallyl-*N*-octadecylamine-*alt*-maleic acid (PDAOM)). The phase state of mixed monolayers on a water surface were studied and the conditions for transferring them onto solid supports were determined. The spectral and luminescent properties of LB films were also studied.

EXPERIMENTAL

All of our dyes were prepared according to the procedure described in [14].

3-Diethylamino-7-imino-7H-chromen[3',2'-3,4]pyrido[1,2-a]benzimidazole-6-carbonitrile (dye **I**) was prepared via the interaction between iminocoumarin-7 and maleic nitrile in isobutanol; 3-diethylamino-7-oxo-7-oxo-7H-chromeno[3',2'-3,4]-pyrido [1,2a]benzimidazole-6-carbonitrile (dye **II**) was prepared via the interaction between dye **I** and concentrated hydrochloric acid at 100°C over 3 h. Synthesis details and a description of PDAOM can be found in [15–16].



R = NH—dye I

R = O—dye II

Monolayers were formed on a water surface in a Langmuir bath. The surface pressure was measured using Wilhelmi scales that allowed us to register surface tension in the range of 0 to 100 mN/m with an accuracy of up to 0.1%. The rate of monolayer compression in measuring the curves of the dependence of surface pressure on the molecular area and upon transferring monolayers onto a solid support prepared from nonluminescent quartz was 0.02 mm/s.

Deionized water purified using an AquaMax water purification system was used as our subphase. The specific water resistance was 18.2 MΩ/cm, demonstrating its high purity. The surface pressure was 72.8 mN/m at pH 5.6 and a temperature of 22°C.

The investigated monolayers were formed on the surface of subphase by spreading from solution. The polymer was dissolved in an ethanol/chloroform mixture in a volume ratio of 1 : 4. The dyes were dissolved in chloroform and mixed with polyampholyte in the required ratios. The relative concentration of luminophors was 10, 33, and 50 mol %. The monolayers were transferred onto solid supports by Y-type vertical lift at surface pressure $\pi = 21$ mN/m.

We studied the stability of mixed monolayers by tracking changes of surface tension over time in a constant monolayer area to determine if it was possible to maintain the required monolayer density when transferring it onto a solid support [17]. Substantial changes in surface pressure were observed for all monolayers during their first 10 min. The surface pressure did not change appreciably in the following 60 min.

Absorption spectra were registered on a Hewlett-Packard 8453 spectrophotometer, while fluorescence spectra were measured on a Cary Eclipse Varian spectrofluorimeter equipped with a xenon lamp as the excitation source. The fluorescence quantum yields (φ_{fl}) of the dyes were measured using rhodamine 6G ($\varphi_{fl} = 0.94$) and rhodamine C ($\varphi_{fl} = 0.70$) ethanol solutions as standards at equal excitation intensities λ_{ex} , thereby obtaining spectra that were normalized to standard fluorescence intensity.

The spectral and kinetic parameters of the samples were measured on a spectrofluorimeter with registration in the photon counting regime. The registration part of the instrument was a H7421 photomultiplier and a Hamamatsu M8784 counting board. The samples were placed in an evacuating optical cryostat to conduct investigations over a wide range of tempera-

tures. Photoexcitation was performed using ATC-350 laser radiation ($\lambda_{gen} = 532$ nm, $P = 8$ W). In measuring the kinetics of delayed fluorescence, we used a system consisting of a mechanical rotating optical shutter that closed the registration monochromator's slit at the moment of the laser pulse to eliminate the signal of ordinary fluorescence. Measurements began 10 μ s from the moment of laser pulse arrival. No fewer than 2000 acquisitions were needed to obtain a signal of reasonable level. A computer controlled the instrument, the acquisition of signals, and their further processing.

RESULTS AND DISCUSSION

Phase States of Monolayers on a Water–Air Interface

Figure 1 shows the isotherms from the monolayer compression of dyes I and II, along with those for PDAOM on a water–air interface that describe the dependence of surface pressure (π) on specific area (A) for one molecule of a mixed monolayer. The phase states of individual polyampholyte monolayers were studied earlier and described in [16].

Figure 1 shows that the individual monolayers of dyes on a water surface are basically in the liquid state (Fig. 2, curves 5 and 5'). Instability and irregularity of spreading on subphase surface are characteristic for all unmixed monolayers of the investigated dyes. Extrapolating the curve to zero allowed us to determine the molecular area within monolayer limits of 0.32 nm² for dye I and 0.33 nm² for dye II, respectively. Simulation in the force field MM2 showed [18] that this area corresponds to when the long axis of a dye molecule is in contact with a subphase surface.

A mixed solution of amphiphilic polyampholyte and dye allowed us to obtain more stable and condensed films on the water surface. The surface pressure began to rise with smaller specific areas per single molecule. Isotherms also assumed a steeper form, repeating that of the compression curve of the PDAOM monolayer. Our compression diagram shows that not only is a gas phase in the surface pressure range of 0 to 2 mN/m characteristic of all our mixed monolayers of dyes and amphiphilic polymer, but a transition to the liquid condensed state as well. The mixed monolayers collapse at π values close to 30 mN/m. As the concentration of luminophore molecules in the monolayers increases, the molecular area shrinks, indicating

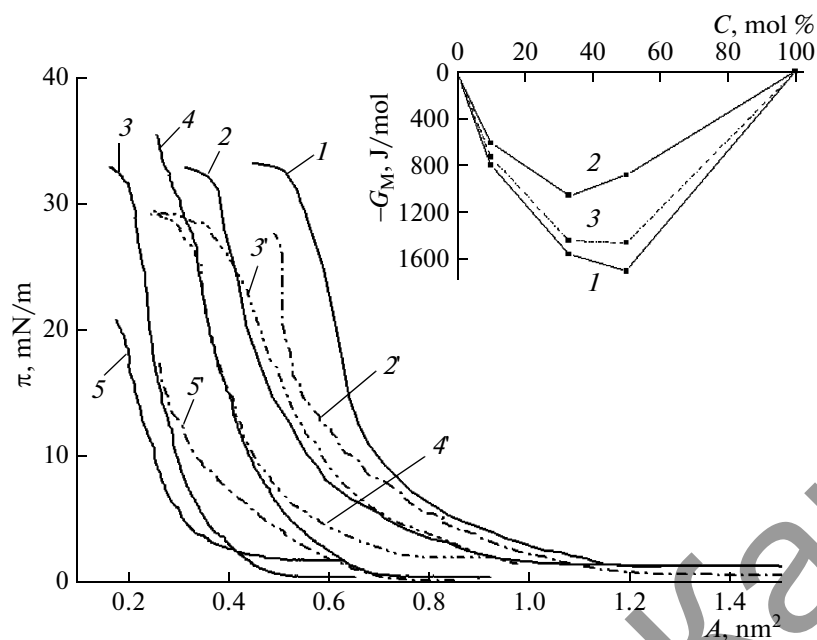


Fig. 1. Compression isotherms for monolayers of dyes I (curves 2–5) and II (curves 2'–5'), and PDAOM at following dye concentrations: (1) is 0; (2, 2') is 10; (3, 3') is 33; (4, 4') is 50; and (5, 5') is 100 mol %. The insert gives the calculated values of the Gibbs mixing energy ($\pi = 0–20$ mN/m): (1) is curve G_1 ; (2) is curve G_M of dye I; (3) is curve G_M of dye II.

denser dye and polyampholyte molecular packing dye to incorporating dye molecules between the ineffective packed octadecyl radicals of the polymer [16].

We calculated the Gibbs free energy to assess the nature of intermolecular interaction between chromens and PDAOM in the forming monolayers along with their thermodynamic stability. Information on the miscibility of mixture components and their aggregation can be obtained by calculating the Gibbs energy (G_M). The increase in Gibbs free energy was estimated from the π – A isotherms using the equations [19, 20]

$$G_1 = RTN_1(\ln N_1) + RTN_2(\ln N_2), \quad (1)$$

$$\Delta G_E = \int_0^\pi (A_{12} - N_1A_1 - N_2A_2) d\pi, \quad (2)$$

and

$$G_M = G_1 + \Delta G_E, \quad (3)$$

where ΔG_E is the increase in the Gibbs energy of mixing, G_1 is the Gibbs energy of mixing for an ideal system, and G_M is the actual Gibbs energy of mixing; A_1 , A_2 , A_{12} are the average areas per one molecule in monolayers of pure dye, pure polyampholyte, and in a mixed film, respectively, at a given π value; and N_1 and N_2 are the mole fractions of dye and polyampholyte, respectively.

The insert in Fig. 1 shows the dependences of the Gibbs energy on the dye's concentration within a monolayer. Our data show that the free energy of mixing is distinct from zero for all of the dye–polyam-

pholyte ratios, demonstrating the immiscibility of components in a monolayer. The negative value of the increase in Gibbs energy also indicates the repulsive nature of dye and PDAOM molecular interaction [20], which could stimulate the formation of aggregates or microcrystals even within a mixed monolayer [19].

Absorption and Fluorescence Spectra

The absorption and fluorescence spectra of ethanol solutions and mixed LB films of polyampholyte polymer and dye I are presented in Fig. 2a. The longwave absorption spectrum of the ethanol–dye solution (curve 1) is a broad band in the range of 450 to 600 nm that contains two distinct maxima at 517 and 551 nm. The fluorescence spectrum of dye I in ethanol (curve 1') has a maximum at a wavelength of 573 nm and an ill-defined shoulder in the range of 615 to 630 nm. The position of the fluorescence spectrum and its form do not depend on the excitation wavelength. The fluorescence quantum yield of dye I in ethanol is 0.99, relative to the ethanol solution of rhodamine 6G ($\phi_{fl} = 0.94$) used as our standard.

The shortwave maximum in the absorption spectrum at $\lambda_{max}^{abs} = 517$ nm is a mirror image of the fluorescence spectrum shoulder in the wavelength range of 515 to 530 nm, confirming the vibrational nature of these side maxima [21]. Our data show that the spectra of absorption and fluorescence in ethanol are produced by monomeric molecules.

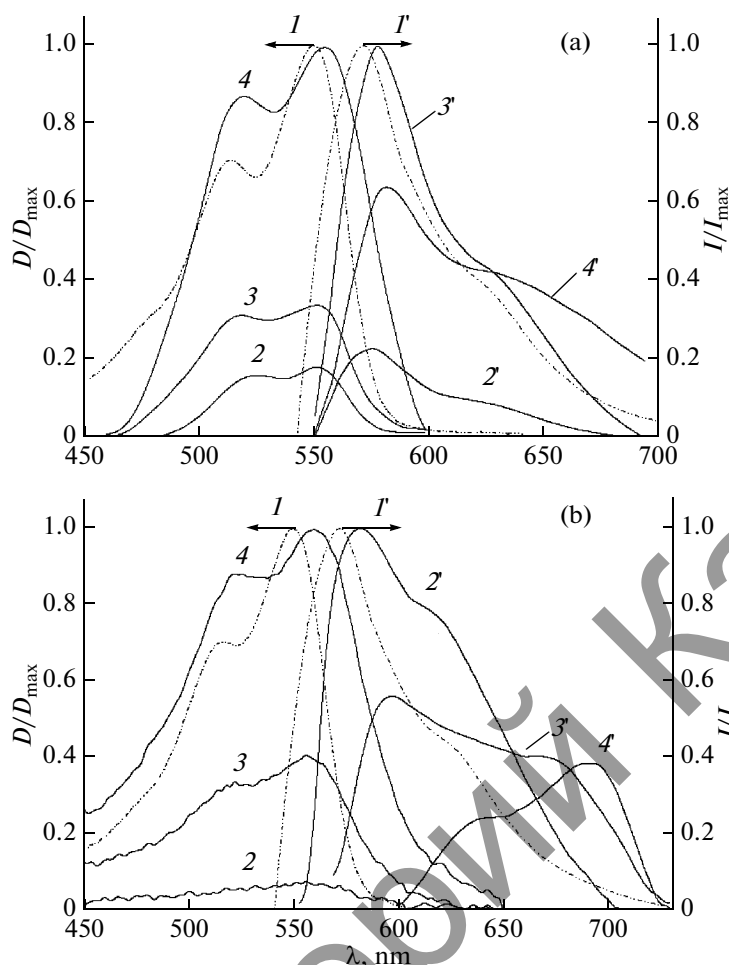


Fig. 2. Absorption (1–4) and fluorescence (1'–4') spectra of dye (a) I and (b) II in ethanol (1, 1') and mixed LB films of dye and polyampholite at various concentrations of dye: 10 (2, 2'), 33 (3, 3'), 50 mol % (4, 4').

The absorption spectra of LB films of dye I (curves 2–4) are broad bands with two maxima at 520 and 556 nm. The maxima of the spectra are shifted in the longwave region relative to the maximum of absorption spectrum in ethanol. The half-breadth of the film absorption spectrum for dye concentration $C_d = 10$ mol % is $\Delta\lambda_{1/2}^{\text{abs}} = 74$ nm, which is close to that of the absorption spectrum for dye in ethanol, $\Delta\lambda_{1/2}^{\text{abs}} = 70$ nm. The half-breadth of the absorption spectrum increases as the concentration of dye in the film rises. The half-breadth of the absorption spectra is 80 and 82 nm for dye concentrations in films of 33 and 50 mol %, respectively. With an increase in the concentration of luminophore molecules in the LB film, we observe stronger optical density in the dye absorption band.

The fluorescence spectra of the LB films (curves 2'–4') were measured upon sample excitation at $\lambda_{\text{ex}} = 520$ nm. A band with a maximum at 577 nm and a half-breadth of $\Delta\lambda_{1/2}^{\text{fl}} = 46$ nm was found for the

film with $C_d = 10$ mol %. As with ethanol solutions, the fluorescence spectra of the LB films have an ill-defined shoulder in the range of 620 to 640 nm. The fluorescence spectra are bathochromic shifted as dye concentration rises in the monolayer. The maximum of the fluorescence spectrum lies at 580 nm for the LB film with a concentration of 33 mol % and at 583 nm for the film with dye concentration of 50 mol %. Fluorescence quenching and an increase in band half-breadth ($\Delta\lambda_{1/2}^{\text{fl}} = 84$ nm) is observed at $C_d = 50$ mol %. The shortwave part of the spectrum (monomer fluorescence) is quenched most strongly.

In LB films, the proximity of particles results in the evolution of molecular aggregation [22]. In LB films with dye I, aggregation is also observed with a rise in molecule concentration. The broadening of the absorption and fluorescence spectra, the bathochromic shift of the fluorescence maximum, and the relative increase in the fluorescence of aggregates in the longwave part of the radiation spectrum support this conclusion.

The absorption and fluorescence spectra of dye **II** in ethanol (Fig. 2b, curves 1 and 1') with maxima at $\lambda_{\max}^{\text{abs}} = 550$ nm and $\lambda_{\max}^{\text{fl}} = 573$ nm exhibit a vibronic structure. The quantum yield of fluorescence measured relative to our standard of rhodamine C ($\phi_{\text{fl}} = 0.70$) was 0.75.

The absorption spectra of dye **II** in LB films (Fig. 2b, curves 2–4) are also broad bands with two maxima at 522 and 560 nm, shifted toward the long-wave side relative to the absorption spectrum of dye in ethanol solution. The half-breadth and optical density of the absorption bands increase as the concentration of dye in the film rises.

Substantial changes were observed in fluorescence spectra (Fig. 2b, curves 2'–4') if the dependence of the absorption spectra of LB films on concentration was similar for dyes **I** and **II**. The most intense fluorescence is displayed by films with dye concentrations of $C_d = 10$ mol % (Fig. 2b, curve 2'). The spectrum with a maximum at wavelength $\lambda_{\max}^{\text{fl}} = 583$ nm is close in shape to that of the ethanol–dye solution. The band half-breadth is $\Delta\lambda_{1/2}^{\text{fl}} = 94$ nm, while it is $\Delta\lambda_{1/2}^{\text{fl}} = 51$ nm for the ethanol solution. Fluorescence quenching and a longwave shift of the band occurs as the concentration of dye rises (curves 3' and 4'). The mirror symmetry of the absorption and fluorescence spectra is broken at dye concentrations of 33 and 50 mol %.

The reason for such behavior of the fluorescence spectra could be dye molecule aggregation. Molecular aggregation is, however, first manifested in electronic absorption spectra as a rule [23]. As is evident from Fig. 2b, the apparent correlation between the absorption and fluorescence spectra disappears at high dye concentrations. Analysis of the absorption spectra allow us to argue for the presence of dye **II** aggregates in LB films to the same extent as for dye **I**.

Under conditions of dense molecular packing in LB layers, excimers can emerge out of dimeric states and be detected from their characteristic longwave fluorescence [22, 23]. We may assume that the red shift observed in the fluorescence spectra of LB films of dye **II** is associated with the formation of dye excimers.

ACKNOWLEDGMENTS

This work was supported by the Kazakhstan Ministry of Education and Science, project no. 1196/GF.

REFERENCES

1. A. A. Eliseev and A. V. Lukashin, *Functional Nanomaterials*, Ed. by Yu. D. Tret'yakov (Fizmatlit, Moscow, 2010) [in Russian].
2. A. G. Vitukhnovsky, M. I. Sluch, J. G. Warren, and M. C. Petty, *Chem. Phys. Lett.* **173**, 425 (1990).
3. A. K. Dutta, T. N. Misra, and A. J. Pal, *Langmuir* **12**, 359 (1996).
4. S. Acharya, D. Bhattacharjee, and G. B. Talapatra, *J. Colloid Interface Sci.* **244**, 313 (2001).
5. G. A. Biesmans, G. Versbeek, B. Verschuere, et al., *Thin Solid Films* **169**, 127 (1989).
6. F. Embs, D. Funhoff, A. Laschewsky, et al., *Adv. Mater.* **3**, 25 (1991).
7. A. Laschewsky, *Eur. Chem. Chronicle* **2**, 13 (1997).
8. V. V. Arslanov, *Russ. Chem. Rev.* **60**, 584 (1991).
9. V. I. Zemskii, Yu. L. Kolesnikov, and I. K. Meshkovskii, *Physics and Technology of Pulsed Dye Lasers* (SPbGU ITMO, St. Petersburg, 2005) [in Russian].
10. F. Bayrakceken, A. Yaman, and M. Hayvali, *Spectrochim. Acta* **61**, 983 (2005).
11. M. Ahmad, T. A. King, D.-K. Ko, et al., *Opt. Laser Tech.* **34**, 445 (2002).
12. R. Schiener, H. Pillekamp, M. Kerscher, and R. U. Peter, *MMW Fortschr. Med.* **145** (8), 45 (2003).
13. R. Giri, *Spectrochim. Acta A* **60**, 757 (2004).
14. V. I. Alekseeva, O. L. Kaliya, E. A. Luk'yanets, et al., Patent RF No. 2095384.
15. F. Rullens, M. Divillers, and A. Laschewsky, *Macromol. Chem. Phys.* **205**, 1155 (2004).
16. S. A. Yeroshina, N. Kh. Ibrayev, S. E. Kudaibergenov, et al., *Thin Solid Films*, No. 516, 2109 (2008).
17. V. V. Arslanov, *Russ. Chem. Rev.* **69**, 883 (2000).
18. T. Clark, *A Handbook of Computational Chemistry A* (Wiley, New York, 1985).
19. S. Acharya, T. Kamilya, J. Sarkar, et al., *Mat. Chem. Phys.* **104**, 88 (2007).
20. M. Kodama, O. Shibata, Sh. Nakamura, et al., *Colloids Surf. B* **33**, 211 (2004).
21. A. N. Terenin, *Photonics of Molecules of Dyes and Related Organic Compounds* (Nauka, Leningrad, 1967), p. 616 [in Russian].
22. N. Kh. Ibraev, A. M. Zhunusbekov, and D. Zh. Satybal-dina, *Opt. Spectrosc.* **87**, 298 (1999).
23. V. I. Yuzhakov, *Russ. Chem. Rev.* **61**, 613 (1992).

Translated by E. Kapinus